Medical & Biological Engineering & Computing (2021) 59:621–632
https://doi.org/10.1007/s11517-021-02314-0

ORIGINAL ARTICLE

Classification of orthostatic intolerance through data analytics

Steven Gilmore[1] · Joseph Hart[2] · Justen Geddes[1] · Christian H. Olsen[3] · Jesper Mehlsen[4] · Pierre Gremaud[1] · Mette S. Olufsen[1]

Received: 19 March 2020 / Accepted: 15 January 2021 / Published online: 13 February 2021

Abstract

Imbalance in the autonomic nervous system can lead to orthostatic intolerance manifested by dizziness, lightheadedness, and a sudden loss of consciousness (syncope); these are common conditions, but they are challenging to diagnose correctly. Uncertainties about the triggering mechanisms and the underlying pathophysiology have led to variations in their classification. This study uses machine learning to categorize patients with orthostatic intolerance. We use random forest classification trees to identify a small number of markers in blood pressure, and heart rate time-series data measured during head-up tilt to (a) distinguish patients with a single pathology and (b) examine data from patients with a mixed pathophysiology. Next, we use Kmeans to cluster the markers representing the time-series data. We apply the proposed method analyzing clinical data from 186 subjects identified as control or suffering from one of four conditions: postural orthostatic tachycardia (POTS), cardioinhibition, vasodepression, and mixed cardioinhibition and vasodepression. Classification results confirm the use of supervised machine learning. We were able to categorize more than 95% of patients with a single condition and were able to subgroup all patients with mixed cardioinhibitory and vasodepressor syncope. Clustering results confirm the disease groups and identify two distinct subgroups within the control and mixed groups. The proposed study demonstrates how to use machine learning to discover structure in blood pressure and heart rate time-series data. The methodology is used in classification of patients with orthostatic intolerance. Diagnosing orthostatic intolerance is challenging, and full characterization of the pathophysiological mechanisms remains a topic of ongoing research. This study provides a step toward leveraging machine learning to assist clinicians and researchers in addressing these challenges.

Keywords Orthostatic intolerance · Syncope · Classification · Clustering · Machine learning

1 Introduction

Cerebral hypoperfusion is usually caused by a decrease in arterial blood pressure (BP) to a level below the autoregulatory capacity giving rise to symptoms including dizziness, nausea, blurred vision, and eventually syncope (or fainting—loss of consciousness from 10 to 20 s with spontaneous recovery [9]). Arterial BP falls when cardiac output and/or systemic vascular resistance are reduced—usually by a sudden pause in the heart rhythm or loss of arteriolar tone. Both can cause syncope, but in many patients, symptoms result from a combination of the two pathophysiological responses [16, 35]. It is estimated that 25% of the population experience syncope and even more feel lightheaded or dizzy at some point in their life and these symptoms account for over 1 million visits to emergency departments per year in the USA alone [31]. A standard diagnostic procedure includes the head-up tilt (HUT) test continuously measuring heart rate (HR) and arterial BP.

Several studies advocate the HUT test as the diagnostic method of choice due to its high diagnostic yield [7, 15], but correct analysis of recorded signals requires expertise in the field, not always available in emergency clinics. The HUT test provides information about the integrated cardiovascular response via measurements of HR and BP. However, analyses of these signals are often limited to simple steady-state quantities including mean BP and HR,

✉ Mette S. Olufsen
msolufseg@ncsu.edu

1 North Carolina State University, Raleigh, NC, 27695, USA

2 Sandia National Laboratories, Albuquerque, NM, 87123, USA

3 Novo Nordisk A/S, 2880 Bagsværd, Denmark

4 Rigshospitalet, University of Copenhagen, 2100, Copenhagen Ø, Denmark

pulse pressure, and the HR change between rest and HUT, omitting critical information embedded in the signals' dynamics interaction.

The most prevalent form of orthostatic intolerance is reflex activation of the autonomic nervous system, subclassified phenomenologically based on induced changes in BP or HR [4, 26, 27, 40]. For patients with orthostatic intolerance, the HUT test is performed to reproduce their neurally mediated reflex in a controlled setting. The HUT test induces pooling of blood below the diaphragm and a subsequent decrease in venous return. For healthy controls, homeostasis is re-established by triggering the baroreflex, which increases HR, cardiac contractility, and peripheral vascular resistance. Prolonged time in the upright position (> 40 min) without the ability to activate the muscle pump will induce reflex syncope (often referred to as vasovagal syncope). If patients cannot be diagnosed within the first 20 min of HUT, to distinguish controls and patients with orthostatic intolerance, additional stimulation is induced by administering nitroglycerine, a vasodilator, which in turn increases HR above the regulatory limit.

Patients are diagnosed with postural orthostatic tachycardia (POTS) if they experience chronic orthostatic intolerance within the first 10 minutes of HUT, resulting in an HR increase of more than 30 bpm (> 40 bpm in individuals aged 1219 years) with little or no change in BP [39]. Patients whose BP falls before HR and where HR falls to a ventricular rate of less than 40 bpm for more than 10 s, without asystole of more than 3 s, are classified as cardioinhibitory (type 2A) [5], and patients experiencing a rapid fall in BP with no or minor HR changes are classified as vasodepressive [6, 27]. If both conditions are present, patients are classified as mixed. For each group, these disease characteristics are often combined with frequent episodes of lightheadedness, palpitations, tremulousness, generalized weakness, blurred vision, exercise intolerance, or fatigue in the upright position [10, 39].

Figure 1 shows examples of each subject type: control, POTS, cardioinhibition, vasodepression, and mixed. The figure includes two patients experiencing a mixed syncope; one patient primarily experiencing vasodepression and one patient primarily experiencing cardioinhibition.

Several pathways could be modulated by these reflex responses, but little is known about the precise hemodynamic maladjustments causing these reactions; and hence, it is challenging to generate targeted treatments. The identification of precise pathways requires a more detailed classification of patient groups.

This study demonstrates how machine learning can be used to assist clinicians in classifying patients with orthostatic intolerance providing more insight into what features are the most important for identifying different disease subgroups. We focus on four types of abnormal responses, including POTS, cardioinhibition, vasodepression, and mixed vasodepression and cardioinhibition (in the remainder of this study, we refer to the latter group as "mixed"). These groups were chosen since they comprise most patients referred to the syncope center at Bispebjerg and Frederiksberg Hospitals, Denmark, from which data have been made available.

2 Data and methods

This study analyzes anonymized retrospective data from 186 subjects distributed in five groups: controls and patients with POTS, cardioinhibition, vasodepression, and mixed syncope. All subjects were diagnosed using a HUT test, examining their ability to control BP and HR. Data extracted from health records were collected between 2004 and 2015 at the syncope clinic at Bispebjerg and Frederiksberg Hospitals, Denmark. All subjects were referred to the clinic after experiencing dizziness, lightheadedness, or syncope. Subjects were diagnosed in the clinic and those who did not show any symptoms were categorized as controls. For all subjects, cardiovascular disease was ruled out prior to testing, and no patients received medication at the time of the study. The data-handling committee at Bispebjerg and Frederiksberg Hospitals approved the analysis of the anonymized retrospective data.

2.1 Head-up tilt test

After arriving at the hospital, all subjects were instrumented with BP and electrocardiogram (ECG) sensors. BP was measured using a Finapres device (Finapres Medical Systems B.V.) in the index finger of the non-dominant hand. The hand was placed in a sling at the level of the heart. ECG was recorded using standard precordial leads. Continuous ECG and BP signals were sampled at a rate of 1000 Hz and saved digitally using an A/D-converter communicating with a computer via LabChart 7 (ADInstruments). This program allows the extraction of HR from the ECG measurement. After steady signals were detected, following recommendations by Bartoletti et al. [1], the subjects rested for 10 min in the supine position before being tilted head-up to an angle of 60° at a speed of 15°/second measured by way of an electronic marker. The table remained tilted up during the initial passive phase of the test. In the case of a negative passive response, after approximately 20 min in the upright position, a provocative drug—nitroglycerine—was administered to induce a neural reflex (an example is shown in Fig. 1). For POTS patients, their diagnosis was established within the first 10 min of head-up tilt, and therefore they were not given nitroglycerine. All patients

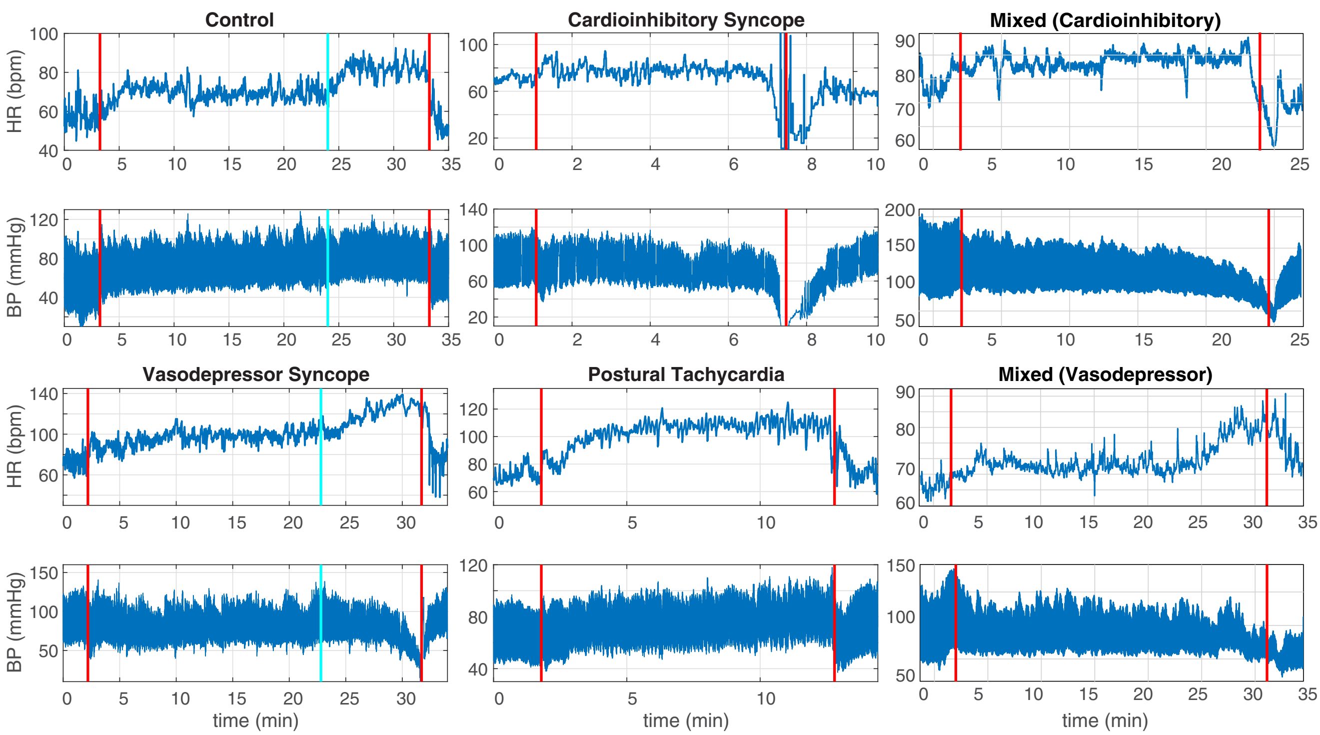

Fig. 1 Example data from the HUT test for six subjects: a healthy control and patients with POTS, cardioinhibitory syncope, vasodepressive syncope, and mixed cardioinhibition and vasodepression syncope. For the latter patient group, we show two examples, a patient primarily experiencing cardioinhibition and one primarily experiencing vasodepression. The red line lines denote the start and end of the tilt from the supine position, up to 60° and back to the supine position. Heart rate (beats per minute) and BP (mmHg) are displayed as functions of time. The light blue lines denote time for administration of nitroglycerine, a vasodilator

and controls were returned to the supine position at the same tilt speed after a total of 30 min or earlier if they presented signs of syncope or presyncope.

2.2 Data and clinical classification

For each subject, time-series measurements of HR and BP are available over the course of the HUT test. Our analysis is based on data starting 2 min before the tilt-up and lasting until 2 min after the tilt-down. The duration of the test varies for each subject, and thus so do the lengths of the time-series. We denote by p_i the number of samples taken for subject i, $i = 1, \ldots, 186$. The time-series data for the i^{th} subject are denoted by:

$$h^i = (h^i_1, h^i_2, \ldots, h^i_{p_i}),$$
$$b^i = (b^i_1, b^i_2, \ldots, b^i_{p_i}),$$

where h and b refer to HR and BP, respectively. Each subject was classified by a clinician as either *control* or symptomatic, experiencing *POTS*, *cardioinhibitory syncope*, *vasodepressive syncope*, or *mixed syncope* (see Fig. 1 and text below). The distributions are reported in Table 1, and summary statistics for the HR and BP measurements are given in Table 2. This table reports the mean HR and BP ±1 standard deviation calculated at rest (before HUT), during the first 50% and last 25% of the HUT. Patients not displaying a response to the tilt in less than 20 min, nitroglycerine was administered sublingually at a dose of 0.4 mg; it was given to 94% of the control subjects and 0%, 64%, 78%, and 76% of the POTS, cardioinhibitory, vasodepressive, and mixed patients.

Controls include subjects admitted to the syncope clinic at Bispebjerg and Frederiksberg Hospitals, Denmark, who had a typical outcome when testing their autonomic nervous system.

Table 1 Summary of subject distribution

Class	Subjects	Age range	Age mean/median	Female (%)
Control	89	14–92	50/49	67
POTS	13	16–38	24/22	85
Cardioinhibition	28	15–80	33/31	63
Vasodepression	27	67–91	58/63	67
Mixed	29	17–92	50/51	70

Table 2 Mean values ±1 standard deviation of HR and BP at rest and during the beginning (phase I) and end (phase II) of the HUT test

Class	Rest	Tilt phase I	Tilt phase II
Mean heart rate (HR)			
Control	70±12	78±13	93±17
Cardioinhibition	67±12	78±14	83±21
Vasodepression	70±10	79±13	87±17
POTS	69±15	98±14	105±19
Mean blood pressure (BP)			
Control	76±16	89±17	88±18
Cardioinhibition	76± 7	89±10	83±14
Vasodepression	82±17	90±17	81±16
POTS	67±8	74± 7	77± 7

Phase I includes averages over the first 50% of the tilt interval and *Phase II* includes averages over last 25% of the tilt interval

POTS patients may experience dizziness and lightheadedness, but typically do not faint [39] (none of the POTS patients included in this study fainted). These patients may have a reduced central blood volume causing blood pressure regulation to be challenged by changes in intrathoracic pressure due to respiration. This causes pathological fluctuations in blood pressure with phase-shifted heart rate changes elicited by the baroreceptor control system. POTS patients typically have excessive vagal withdrawal leading to inappropriate increases in heart rate by more than 30 beats per minute (>40 bpm in individuals aged 12–19 years), which further reduces cardiac filling due to a shortening of the diastolic filling time. As a result, the heart rate increases while blood pressure oscillates [11].

Cardioinhibitory syncope is caused by excessive pooling of blood in the extremities with few presyncopal conditions, combined with an extreme slowing of HR (bradycardia) or temporary cardiac pause (asystole) of at least 5 s [6, 26]. The drop in HR is followed by a rapid fall in BP occurring within a few missed heartbeats for most patients. The result is decreased venous return, reducing the filling of the left heart. The reduced filling of the left heart likely causes the ventricular walls to touch in systole, eliciting the so-called Bezold Jarisch reflex [25, 38], stimulating pressure receptors in the ventricular wall.

Vasodepression syncope is also caused by excessive pooling of blood in the extremities. These patients experience a withdrawal of sympathetic activity, leading to peripheral vasodilatation and a more gradual fall in BP, giving presyncopal symptoms. For patients with this condition, the drop in BP is slower, allowing prominent presyncopal symptoms, including lightheadedness, nausea, dizziness, and visual blurring. For these patients, the Bezold Jarisch reflex likely inhibits sympathetic vasoconstriction resulting in a significant drop in BP, which may or may not be followed by a drop in HR, eventually inducing the syncope.

Mixed syncope patients typically experience both cardioinhibition and vasodepression. Figure 1 shows two examples of patients with mixed symptoms. One patient primarily exhibits cardioinhibition, and one patient primarily exhibits vasodepression.

The classification corresponding to the above expert diagnosis is denoted Y^i, $i = 1, \ldots, 186$. For any patient, Y^i takes values in the five classes introduced in the previous paragraph. The complete data is thus contained in the set

$$\{h^i, b^i, Y^i\}_{i=1}^{186}.$$

The time-series are first subsampled at 20 Hz, down from 1,000 Hz in the original signal. Second, the signals are preprocessed using a moving average window with a width of 1,000 points (or equivalently 50 s). Finally, we normalized each signal by subtracting its global mean for each subject. We denote the preprocessed normalized time series by $\mathcal{H}^i$ and $\mathcal{B}^i$ where

$$(\mathcal{H}^i, \mathcal{B}^i) \in \mathbb{R}^{N^i} \times \mathbb{R}^{N^i}, \qquad i = 1, \ldots, 186,$$

with N^i referring to the number of retained sample values for the i^{th} subject.

2.3 Random forest classifier

We use Random Forests [2, 17] (also called Random Decision Forests) an ensemble learning method for classification. This method constructs a large number of decision trees operating as an ensemble. Each tree outputs a class prediction, and the algorithm selects the best solution by means of voting. We use the implementation encoded in the R RANDOMFOREST function.

The goal of our classification is twofold: (i) to determine a subset of the data that can distinguish the patients, and (ii) to explore the similarity between the mixed syncope and the other three classes. To achieve our first goal, we focus on the 157 patients with a single pathology (i.e., we do not include patients with mixed cardioinhibition and vasodepression symptoms) and choose the markers that maximize the classification rate. Below, we show that high classification rates can be obtained by restricting these markers to simple time sampling of both the normalized HR and BP signals $(\mathcal{H}^i, \mathcal{B}^i)_{i=1}^{157}$.

As illustrated in Fig. 2, for each patient, one marker is placed 1 min before the head-up tilt and another is placed 1 min after the tilt-down. We parameterize the placement

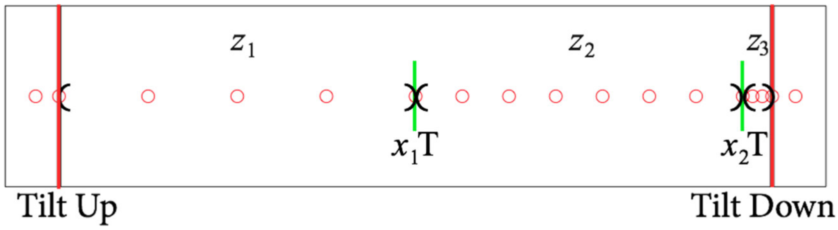

Fig. 2 Marker parameterization: the red lines represent the onset of tilt-up and tilt-down. Markers are placed before and after the tilt, and within the tilt interval (between the red lines). The tilt interval is split into three subintervals $[0, x_1T]$, $[x_1T, x_2T]$, and $[x_2, T]$, where 0 refers to the beginning of the data and T denotes the length of the signal. Each subinterval contains z_i nodes, $i = 1, 2, 3$. The nodes (sample times) are marked by red circles. The first and last intervals. The optimal numerical values for these parameters are $x_1 = 0.4999$, $x_2 = 0.9588$, and $z_1 = 5$, $z_2 = 7$, $z_3 = 3$

of the remaining markers by partitioning the "tilt-up to tilt-down intervals" into three subintervals:

$$[0, x_1T_i], [x_1T_i, x_2T_i], \text{ and } [x_2T_i, T_i],$$

where $0 < x_1 < x_2 < 1$ and T_i denotes the elapsed time between tilts for the i^{th} patient. Next, we place z_j markers uniformly spaced in the j-th subinterval, $j = 1, 2, 3$. For each interval, we retain the sampled values which are the closest in time to

$$\textbf{interval 1:} \quad T^{up} + \ell\, \tfrac{x_1}{z_1-1} T,\ \ \ell = 0, \ldots, z_1 - 1,$$
$$\textbf{interval 2:} \quad T^{up} + (x_1 + \ell\, \tfrac{x_2-x_1}{z_2})T,\ \ \ell = 1, \ldots, z_2,$$
$$\textbf{interval 3:} \quad T^{up} + (x_2 + \ell\, \tfrac{1-x_2}{z_3})T,\ \ \ell = 1, \ldots, z_3,$$

with the conventions that if $z_1 = 0$, there is no node in the first interval and if $z_1 = 1$, the first interval only contains the node corresponding to the tilt up time, T^{up}.

We seek an optimal sampling strategy whereby, within a predefined range, the relative size of the intervals defined by x_1 and x_2 and the numbers of points z_1, z_2, and z_3 in each interval are chosen to maximize the classification rate. More precisely, each choice of $\xi = (x_1, x_2, z_1, z_2, z_3)$ defines a subset of the available data $\mathcal{D}_\xi$ with

$$\mathcal{D}_\xi = \cup_{i=1}^{157} \mathcal{D}_\xi^i,$$

where $\mathcal{D}_\xi^i$ is the subset of the data for the i^{th} subject corresponding to ξ. We construct a cost function through 10-fold cross-validation, namely, $\mathcal{D}_\xi$ partitioned as follows:

$$\mathcal{D}_\xi = \cup_{k=1}^{10} \mathcal{D}_\xi^{\sigma_k} \text{ with } \mathcal{D}_\xi^{\sigma_k} = \cup_{i\in\sigma_k} D_\xi^i,$$

where the σ_k's partition $\{1, \ldots, 157\}$. Algorithm 1 defines a function F which inputs ξ and returns the successful classification rate computed through cross validation on the Random Forest model.

Algorithm 1 Objective function to determine markers.

1: **for** $k = 1$ **to** 10 **do**
2: learn random forest $\mathcal{C}_\xi^k$ on $\mathcal{D}_\xi \backslash \mathcal{D}_\xi^{\sigma_k}$
3: compute r_ξ^k: classification success rate of $\mathcal{C}_\xi^k$ on $\mathcal{D}_\xi^{\sigma_k}$
4: **end for**
5: $F(\xi) = \frac{1}{10} \sum_{k=1}^{10} r_\xi^k$
6:

Note that F inherits the Random Forest model's stochasticity: two calls to F with the same input parameters may lead to two different outputs. However, the stochastic aspect is mostly negligible as numerical experiments indicated that classification rates for the same parameterization have small variations when the model is run multiple times. We used 10-fold cross-validation, which gave a good approximation of the classification rate attained, with leave-one-out cross-validation while allowing for a 20-fold speed-up.

We find the optimal markers by solving the maximization problem:

$$\underset{\xi}{\text{argmax}}\ F(\xi) \text{ subject to } \begin{cases} 0 < x_1 < x_2 < 1, \\ z_i \text{ integer}, i = 1, 2, 3, \\ z_i \geq 0, i = 1, 2, 3, \\ 12 \leq z_1 + z_2 + z_3 \leq 16, \end{cases} \tag{1}$$

where the last constraint is chosen through trial and error; the retained choice balances the amount of information and the associated cost. To maximize F, we first fix z_1, z_2, z_3 and consider the function mapping from $(x_1, x_2) \mapsto F(x_1, x_2, z_1, z_2, z_3)$ as the objective function. We optimized it using the L-BFGS-B option in the R OPTIMX function. This is repeated for every possible combination of z_1, z_2, z_3 satisfying the constraints. The initial iterate is taken as $(.5, .75)$; for all datasets, numerical convergence was reached in 10 iterations or fewer in all cases. The resulting optimal parameterization is given is illustrated in Fig. 2 with optimal numerical values $x_1 = 0.4999$, $x_2 = 0.9588$, and $z_1 = 5$, $z_2 = 7$, $z_3 = 3$.

Results showed that we need 17 nodes (including one pre-tilt and one post-tilt node), i.e., HR and BP data analysis requires 34 nodes (17 BP and 17 HR markers). Moreover, we found that most of the critical information is concentrated immediately before the tilt down. Using the optimal classification rates corresponding to each choice of z_1, z_2, z_3, we compared 605 parameterizations with mean 93%, median 94%, min 69%, and max 97%. Since half of the potential parameterizations give a classification rate between 94 and 97%, we conclude that the classification rate is not sensitive to perturbations in the parameterization.

2.4 Clinical metrics

To determine if machine learning improves classification, we compare results with common clinical metrics used to discern the patient populations. Several of these rely on frequency analysis; therefore, we computed all metrics using data from the first 5 min of the HUT (if available). Five datasets had less than 3 min of HUT data and were not analyzed. To quantify heart rate variability (HRV), we compute the standard deviation of successive differences of RR intervals (SDSD). This measure is one of the most widely used metrics of HRV and is closely related to the standard Poincaré map metrics (SD1 and SD2), which provide a geometric representation of patient heart function in clinical settings [3]. To assess beat to beat baroreflex sensitivity, we use the spontaneous baroreflex method (SBR) [29]. This technique has been shown to provide similar insight as pharmacological methods of baroreflex sensitivity [30]. The above traditional metrics assume stationarity of the signal. However, tachycardia and/or syncope in many of the patient's HUT data suggests that the signals are highly nonstationary. For this reason, we also compute metrics using the uniform phase empirical mode Decomposition [14], which is based on nonstationary signal processing. With this method, we compute the amplitude of the 0.1-Hz component of the HR signal, and the phase difference metric M_h.

3 Results

3.1 Classification

First, we classify the controls and the POTS, cardioinhibitory, and vasodepressive patients. Using the optimal sampling strategy from the optimization problem (1) with leave-one-out cross-validation, we obtain a classification rate of 96%. This result demonstrates the predictive power of the markers and the potential value of machine learning as a complementary tool for syncope diagnosis.

Next, we train the Random Forest on the 157 (non-mixed syncope) subjects and predict the classification of the 29 mixed patients. The Random Forest model classifies these patients using a majority vote over 500 classification trees. The proportion of votes provides a measure of confidence the model has in its classification. Figure 3 shows the subjects plotted using barycentric coordinates of the proportion of votes. The color legend identifies the classification from expert clinicians. All but two controls (98%) were classified correctly. The two "wrongly" classified controls were both termed vasodepressive, likely due to experiencing a slow drop in BP following NG administration; neither patient experienced syncope before being tilted back down. One POTS patient was characterized as a control (a success rate of 92%). This patient experienced an increase in HR of about 20 bpm, below the threshold for POTS. Closer examination of this patient reveals that both HR and BP are oscillating, a characteristic of patients in this group [14]. One patient with cardioinhibition was characterized as a control (a success rate of 96%). As expected for patients in this group, HR fell before BP, but the lag between the drop in HR and BP was shorter for this patient than that for other patients in this group. Two patients diagnosed (by the expert) as vasodepressive were classified as control, with a success rate of 93%. Both patients experienced a fast drop in BP following NG administration, similar to the control group, but fainted—characteristic for patients with vasodepression. Finally, one patient with mixed response was characterized as a control (success rate of 97%). Examining this patient's

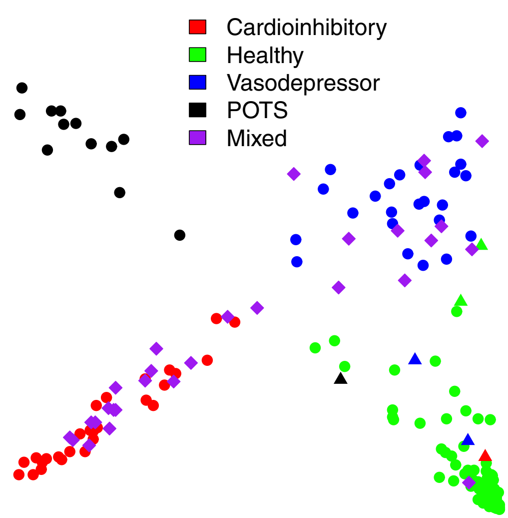

Fig. 3 Barycentric coordinate representation of the classification of four classes and mixed patients (denoted by a ⋄). Misclassified subjects are denoted by a △. Point tightness indicates how well-defined a specific class is

data reveals that neither HR nor BP drops following the tilt; therefore, the HUT is inconclusive for this patient. An important note is that the classification algorithm was able to sub-classify patients with mixed responses in two groups, with 11 patients belonging to the vasodepression group and 17 patients belonging to the cardioinhibition group, picking up differences between patients in this group (illustrated in Fig. 1).

To further analyze classification, we compare heart rate and blood pressure using ANOVA between groups comparing the various parts of the recorded time-series signal. Results (Table 3) show that this analysis can only detect statistically significant differences between the POTS group and other groups. Comparisons of age reveal a difference in age between POTS and cardioinhibitory patients and the control, vasodepression, and mixed patients. We also used a multivariate ANOVA analysis (via the R function MANOVA) comparing the mean HR and BP features reported in Table 2. Results (see Table 4) show that patients in all groups differ from the control group ($p < 0.01$). This analysis also clearly distinguishes POTS patients from cardioinhibition and vasodepression ($p < 0.01$), while it cannot distinguish cardioinhibition from vasodepression.

Finally, pairwise ANOVA comparisons of standard markers described in Section 2.4 and reported in Table 5 reveal that some of the metrics can distinguish POTS and cardioinhibitory from the other patient types, but that none of the metrics can differentiate control, vasodepression, or mixed patients or POTS and cardioinhibitory patients.

Table 3 Pairwise ANOVA analysis ($p < 0.01$) between groups comparing age, the mean blood pressure (BP), and heart rate (HR) at rest, during the first 50% (*Phase I*) and the last 25% (*Phase II*) of the tilt

Metric	Group I	Group II
BP - Phase 0 (Rest)	–	–
BP - Phase I (first 50% of tilt signal)	POTS	Control
BP - Phase II (last 25% of tilt signal)	–	–
HR – Phase 0	–	–
HR - Phase I	POTS	Healthy Vasodepression Cardioinhibitory Mixed
HR - Phase II	POTS	Cardioinhibitory Mixed
Age	POTS	Vasodepression Mixed Control
	Cardioihibitory	Vasodepression Mixed Control

Phase I includes averages over the first 50% of the tilt interval and *Phase II* includes averages over last 25% of the tilt interval

Table 4 MANOVA analysis comparing all the statistics in Table 2 across groups

Group I	Group II
Control	Cardioinhibition
Control	Vasodepression
Control	POTS
Control	Mixed
Cardioinhibition	POTS
Vasodepressor	POTS

The table lists comparisons with p values smaller than the 0.01 threshold

3.2 Clustering

The clustering algorithm, K-means, takes the desired number of clusters, K, as an input argument. To explore possible data structures, we repeat the clustering analysis with various values of K. Clustering results, shown in Fig. 4, are displayed using Silhouette plots [37]. Silhouette values greater than 0 indicate that the patient fits best in its cluster; values less than 0 indicate that it fits better in another cluster. When clustering with $K = 3$, left panel of Fig. 4, we note that the POTS patients are clustered with the controls. This is likely explained by the observation that HR and BP changes following the HUT display similar features (BP and HR do not change significantly, as these patients did not faint). Clustering of patients with single pathology disease with $K = 4$ gives four groups; see the center panel of Fig. 4. Next, for $K = 5$, two different groups of controls emerge (see the right panel of Fig. 4), while the three single pathology groups (patients with POTS, cardioinhibition, and vasodepression) form their own cluster. Finally, taking $K < 3$ or $K > 5$ did not yield any informative cluster structure. We also observed, in agreement with the classification results (see Fig 3), that vasodepression is the most challenging pathology to characterize.

Table 5 Statistically significant comparisons ($p < 0.01$) from pairwise ANOVA comparisons among all five groups via the following methods: standard deviation of successive differences (SDSD), spontaneous baroreflex sensitivity (SBR), and the nonstationary metrics M_h and a_{HR}

Metric	Group I	Group II
SDSD	Cardioinhibitory	Control, vasodepression, mixed
SBR	Cardioinhibitory	Control, vasodepression, mixed
M_h	POTS	Control, vasodepression, mixed
	Cardioinhibitory	Control, mixed
a_{HR}	POTS	Control, vasodepression, mixed

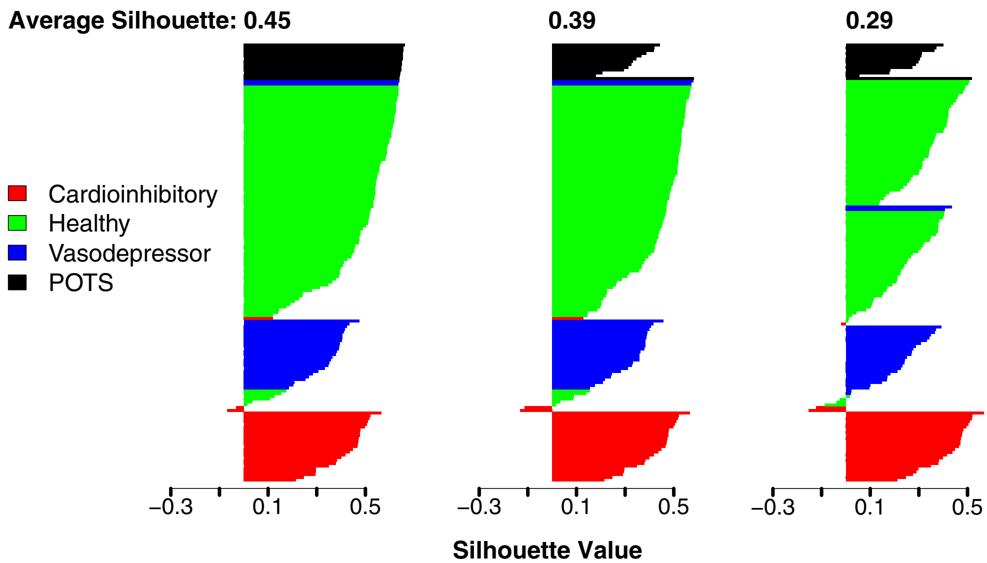

Fig. 4 Silhouette representations of the clustering of the population in 3 (left), 4 (center), and 5 (right) clusters

Further investigation reveals that the two "control" clusters (obtained for $K = 5$) include patients with different features. Figure 5 displays the average (over subjects in the cluster) HR and BP plotted as a function of time. Since the experiment's duration differs slightly for each subject, the horizontal axis in Fig. 5 is a scaled time where the interval between the start and end of head-up tilt is mapped to the interval [0,1].

The vertical lines indicate the position of the markers. We refer to the two clusters as group A and group B. While HR is similar for the two groups, BP differs significantly. Controls in group A, represented by the blue curves, experience a drop in BP following nitroglycerine, while patients in group B, represented by the green curves, do not. It should be noted that the two controls and the two vasodepression patients who have wrongly classified all express features similar to patients in group A

For each group, a representative subject is chosen (A and B). Their HR and BP are displayed in Fig. 6. The differing trends in BP are observed comparing the left and right panels of Fig. 6.

3.3 Traditional metrics

To better judge the results discussed above, we test if data can also be categorized using standard autonomic regulation measures. The specific focus is on analyzing heart rate variability (HRV) and baroreflex sensitivity. These methods can distinguish patients with POTS and cardioinhibition, but not control subjects, patients with vasodepression, or mixed pathologies.

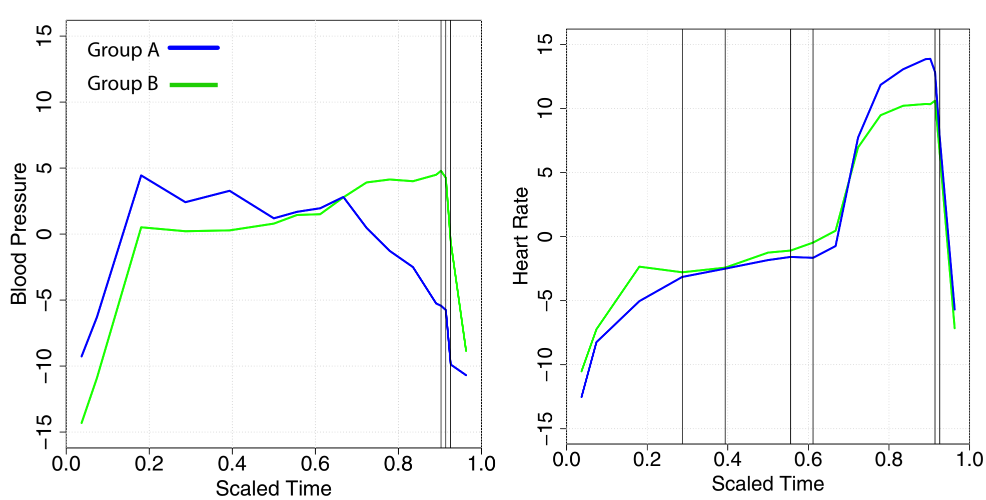

Fig. 5 Normalized BP and HR evolution for the two healthy clusters from Fig. 4; normalized signals are obtained by subtracting the individual global temporal mean from the original signal. Left: BP; the healthy subjects demonstrate two different behaviors; right: HR; the healthy subjects display a similar behavior. Group A and group B are represented by the blue curves and green curves, respectively

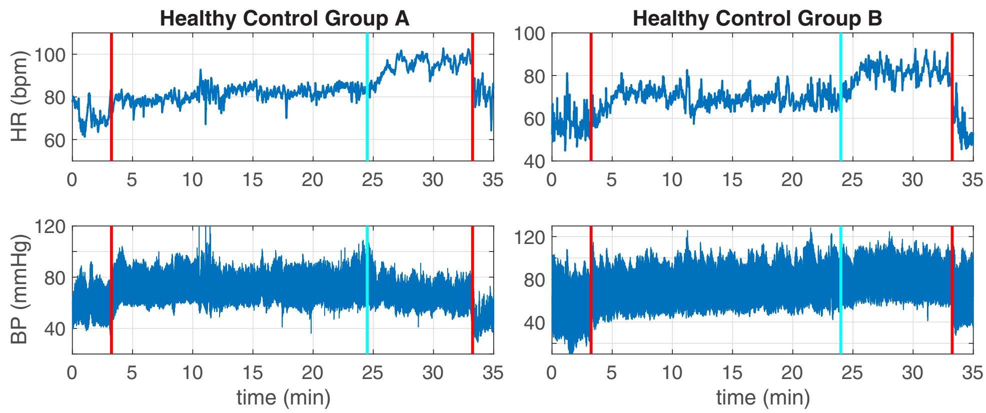

Fig. 6 HR (top) and BP (bottom) for two representative patients from control groups A (left) and B (right)

4 Discussion

This study uses machine learning to classify and cluster patients with orthostatic intolerance manifested as POTS, cardioinhibition, and vasodepression. Data analyzed include HR and BP measurements from a control group and four groups of patients, three single pathology groups, and one mixed group with patients exhibiting cardioinhibition and vasodepression.

Results of our study show that supervised machine learning—here in the form of Random Forests—can differentiate controls and patients with orthostatic intolerance; more specifically, we show that our method can classify more than 93% of all single pathology patients. We also showed that our classification scheme can identify patients with mixed cardioinhibition/vasodepression pathology, a feature we could not determine by simple ANOVA analysis of BP and HR features. Finally, it should be noted that these results were achieved without adding a marker identifying if patients received nitroglycerine.

Of the 186 datasets, only seven patients were classified incorrectly. Of these, we were unable to distinguish between control and vasodepression for five patients. Both pathologies cause a drop in BP after the administration of nitroglycerine. In addition, one patient experiencing cardioinhibition was characterized as a control. For this patient, the HUT did look normal, but the diagnosis may have been based on other tests not analyzed here. One POTS patient was classified as normal, but closer inspection revealed that HR only increased by 20 bpm following HUT, less than the conventional characterization of POTS. However, this patient did exhibit oscillations in both HR and BP, which is common in POTS patients [14, 32, 33] and the patient is therefore likely diagnosed correctly. The machine learning algorithm used in this study is based on an analysis of average BP signals sampled at only 17 points during the tilt protocol and is therefore likely not able to capture this feature.

Findings reported here advance previous studies [19–21, 41], differentiating controls and patients with syncope. Various degrees of success have been reported depending on the type of markers/features considered, e.g., time-domain versus frequency domain, the population size (large versus small), the methods (linear versus non-linear analysis), and the amount of information taken into account. These studies were set up (at least in part) to investigate *early* prediction of syncope, to determine if it is possible to identify patients susceptible to syncope before they faint, i.e., as early as possible during the HUT. However, to our knowledge, no studies were able to identify markers for this purpose. The study reported in this article was not conducted with this question in mind. Nonetheless, our results shed light on this problem.

Analysis of optimal marker location, discussed in Section 2.3, reveals (not surprisingly) that markers placed immediately before the onset of syncope are the most important, i.e., the data collected just before tilt-down, corresponding to interval 3 above, are essential to characterize the disease type. This observation is confirmed by [21], who noted that data analysis from the first 15 min following tilt-up is inadequate for a specific classification of the patient, as the data “miss” that critical time. The results in [41] are encouraging, though they use data in the last minute before syncope in over half of their results.

The focus of this study is on multi-class classification and clustering of syncope data. We are not aware of similar published studies that show similar results. A possible explanation for the dearth of closely related work might be the difficulty of defining these specific classes, as it requires close collaboration with clinicians examining data from a significantly larger cohort of patients.

Unlike other recent analyses of syncope data, such as [19], we do not retain as features quantities explicitly dependent upon the time-frequency analysis of the two signals BP and HR; instead, we sample the signals at optimized times. We tested and observed that the inclusion of “variation dependent features” does not lead to

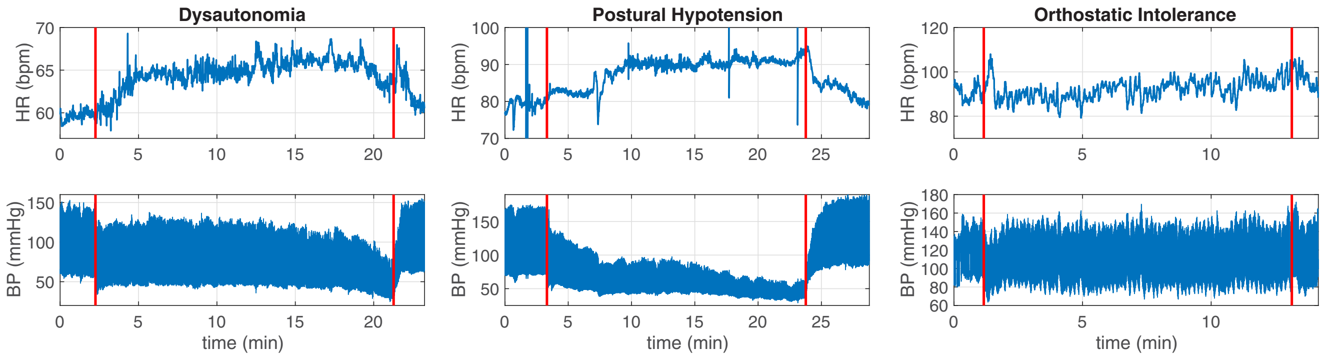

Fig. 7 Additional types of syncope pathologies are not included in this project. Left: dysautonomic response. HUT does not lead to a significant increase in HR, likely due to reduced vagal response; sympathetic system regulation may be intact but cannot keep up with the progressive drop in central blood volume due to capillary filtration of fluid from the intra- to the extravascular compartment. Middle: postural hypotension. HUT causes an excessive drop in BP with some change in HR. This could be due to reduced sympathetic vasoconstriction. The small change in heart rate could be caused by intact vagal stimulation. Right: orthostatic intolerance. During HUT, reduced central blood volume causes BP regulation to be challenged by intrathoracic pressure changes due to respiration. This causes pathological fluctuations in BP with phase-shifted changes in heart rate elicited by the baroreceptor control system

higher classification rates, though we expect that properly chosen quantifiers based on local spectral properties likely can improve our analysis; this is the topic of ongoing investigations. The classification results validate our choice of features and facilitate our understanding of the mixed syncope patients. While clustering largely confirms the validity of our initial clinical classification, it does uncover the existence of two distinct control groups. The two control groups differentiate patients who can maintain BP in response to nitroglycerine versus those who experience a BP drop, though not sufficient to experience presyncope or syncope; all patients in the control group were non-symptomatic (they did not faint). One explanation is that the control subgroup experiences a BP drop following nitroglycerine administration caused by their sympathetic system operating near or at its maximum (before vasodilation induced by nitroglycerine). As a result, these patients may not be able to maintain a high BP through vasoconstriction in response to nitroglycerine.

Overall, our analysis of HR and BP time-series gives a more accurate classification than traditional methods, including HRV (via the standard deviation of successive differences of RR intervals), BRS (baroreflex sensitivity), M_h the phase between heart rate and BP, and a_{HR} the amplitude of the 0.1-Hz heart rate frequency. These methods can distinguish patients with POTS and cardioinhibition, but not control patients, patients with vasodepression, or mixed pathologies. There are many other useful metrics that we did not compute, such as those reported in [12, 13]; however, we chose to examine the above metrics due to their widespread clinical use or their ability to handle nonstationarity.

This study focuses on analyzing HR and BP time-series data measured during HUT, but other physiological signals also impact autonomic function. Examples include respiration [22, 28, 42], cardiac output [24], age [23], and gender [18]. Respiration can be measured directly or determined from the ECG signal by extracting the height of the RR intervals. This approach was used in the study by Randall et al. [32], analyzing data from patients undergoing the Valsalva maneuver. We did not add respiration in the analysis presented here, since it is not measured, and we do not want to add a second identifier extracted from a signal already analyzed. Besides, several modeling studies (e.g., [43]) have shown that adding cardiac output improves prediction. The Finapres can approximate cardiac output, but this estimate is not reliable [34]; and therefore, it was not saved in the patient records. As a result, we could not estimate peripheral resistance, as it relates to BF and BP. Cardiac output can be measured, e.g., using echocardiography, and future studies should examine if adding any of these estimates would improve the classification. While it is not likely that these measures improve the classification success, they may affect marker location and help use fewer data to classify the disease categories.

Tables 2 and 3 show that POTS and cardioinhibition patients are younger than controls, and patients with vasodepression, and mixed a pathophysiology, and that age can be used as a marker to distinguish some pathologies. However, patients included in this study are not age-matched, as data represents the cohort of patients referred to the syncope clinic, and we do not know if the age groups examined are representative for each pathophysiology. Therefore, we did not include this marker in our clustering analysis. Our objective was to include as little data as possible, and even without accounting for age, our algorithm was able to classify most patients correctly. Future work should test if adding age or any of the standard clinical markers would improve the classification.

Finally, the data analyzed are skewed as all patient groups have more female than male participants. This could result from two factors: (a) that females faint more frequently than males (as reported by [8, 18, 36]) or (b) that females may be more likely to seek care when they faint.

In addition to analyzing data from a larger patient cohort, future work will involve the clustering analysis of patients with other pathologies including patients with dysautonomia and postural hypotension (example HR and BP time-series data from representative patients in these groups are shown in Fig. 7). Further research is also necessary to investigate possible pathophysiological characterizations of the above two control groups and potentially include frequency information to identify patients in the POTS group. Moreover, we propose comparing machine learning methodologies (discussed here) with direct mathematical modeling accounting for mechanics in the system. The latter promotes a better understanding of underlying causes leading to observed quantities and facilitates testing of different root causes. Finally, to enable faster diagnoses, we propose to determine how much data is needed for effective classification.

Acknowledgements The authors would like to thank the Statistical and Applied Mathematical Sciences Institute (SAMSI), where this work was initiated, and Peter Novak, Brigham and Women's Hospital, Boston, MA 02115, for helpful discussions.

Funding This work was supported in part by the National Institutes of Health and the National Science Foundation under Grants NSF-DMS 1557761 and NSF-DMS-1745654 and the National Institutes of Health through grant NIH 5P50GM094503-06 VPR sub-award to North Carolina State University.

Declarations

Disclaimer This paper describes objective technical results and analysis. Any subjective views or opinions that might be expressed in the paper do not necessarily represent the views of the U.S. Department of Energy or the United States Government. Sandia National Laboratories is a multimission laboratory managed and operated by National Technology and Engineering Solutions of Sandia LLC, a wholly owned subsidiary of Honeywell International, Inc., for the U.S. Department of Energy's National Nuclear Security Administration under contract DE-NA-0003525. SAND2020-2937 J.

References

1. Bartoletti A, Alboni P, Ammirati F, Brignole M, Del Rosso A, Manzillo G, Menozzi C, Raviele A, Sutton R (2000) The Italian protocol: a simplified head-up tilt testing potentiated with oral nitroglycerin to assess patients with unexplained syncope. Europace 2(4):339–342
2. Breiman L (2001) Random forests. Mach Learn 45:5–32
3. Brennan M, Palaniswami M, Kamen P (2001) Do existing measures of poincaré plot geometry reflect nonlinear features of heart rate variability? Cureus 48(11):1342–1347
4. Brignole M (2007) Diagnosis and treatment of syncope. Heart 93(1):130–136
5. Brignole M, Alboni P, Benditt D, Bergfeldt L, Blanc JJ, Thomsen PB, van Dijk J, Fitzpatrick A, Hohnloser S, Janousek J, Kapoor W, Kenny R, Kulakowski P, Masotti G, Moya A, Raviele A, Sutton R, Theodorakis G, Ungar A, Wieling W (2004) Guidelines on management (diagnosis and treatment) of syncope. Eurospace 6(6):467–573
6. Brignole M, Moya A, de Lange F, Deharoa JC, Elliott M, Fanciulli A, Federowski A, Furlan R, Kenny R, Martin A, Probst V, Reed M, Rice C, Sutton R, Ungar A, van Dijk J (2018) 2018 ESC guidelines for the diagnosis and management of syncope. Eur Heart J 39(21):1883–1948
7. Brignole M, Ungar A, Casagranda I, Gulizia M, Lunati M, Ammirati F, Del Rosso A, Sasdelli M, Santini M, Maggi R, Vitale E, Morrione A, Francese G, Vecchi M, Giada F (2010) Syncope Unit (SUP) investigators: prospective multicentre systematic guideline-based management of patients referred to the syncope units of general hospitals. Europace 12(1):109–118
8. Cubera K, Stryjewski P, Kuczaj A, Nessler J, Nowalany-Kozielska E, Pytko-Polonzyk J (2017) The impact of gender on the frequency of syncope provoking factors and prodromal signs in patients with vasovagal syncope. Przeglad Lekarski 74(4):147–149
9. Ferreira R, da Silva L (2016) The current indication for pacemaker in patients with cardioinhibitory vasovagal syncope. Open Cardiovasc Med J 10:179–187
10. Fletcher J (2020) What to know about vasovagal syncope. https://www.medicalnewstoday.com/articles/327406
11. Fu Q, Vangundy T, Galbreath M, Shibata S, Jain M, Hastings J, Bhella P, Levine B (2010) Cardiac origins of the postural orthostatic tachycardia syndrome. J Am Coll Cardiol 55(25):2858–2868
12. Furlan R, Diedrich A, Rimoldi A, Palazzolo L, Porta C, Diedrich L, Harris P, Sleight P, Biagioni I, Robertson D, Bernardi L (2003) Effects of unilateral and bilateral carotid baroreflex stimulation on cardiac and neural sympathetic discharge oscillatory patterns. Circulation 108(6):717–723
13. Furlan R, Jacob G, Snell M, Robertson D, Porta A, Parris P, Mosqueda-Garcia R (1998) Chronic orthostatic intolerance: a disorder with discordant cardiac and vascular sympathetic control. Circulation 98(20):2154–2159
14. Geddes J, Mehlsen J, Olufsen M (2020) Characterization of blood pressure and heart rate oscillations in pots patients via uniform phase empirical mode decomposition. IEEE Trans Biomed Eng 67(11):3016–3025
15. Greve Y, Geier F, Popp S, Bertsch T, Singler K, Meier F, Smolarsky A, Mang H, Müller C, Christ M (2014) The prevalence and prognostic significance of near syncope and syncope: a prospective study of 395 cases in an emergency department (the speed study). Dtsch Arztebl Int 111(12):197–204
16. Guyton A, Hall J (2016) Medical physiology, 13th edn. Elsevier, Philadelphia
17. Hastie T, Tibshirani R, Friedman J (2009) The elements of statistical learning. Springer Series in Statistics. Springer, New York
18. Jacob G, Barbic F, Glago M, Dipaola F, Porta A, Furlan R (2018) Cardiovascular autonomic profile in women with constitutional hypotension. J Hypertens 36(10):2068–2076
19. Khodor N (2014) Dynamical analysis of mutivariate time series for the early detection of syncope during head-up tilt test. Ph.D. thesis, Université Rennes 1, Rennes, France
20. Khodor N, Carrault G, Matelot D, Amoud H, Khalil M, Boullay N, Carré F, Hernandez A (2016) Early syncope detection during head up tilt test by analyzing interactions between cardio-vascular signals. Dig Signal Process 49:86–94
21. Klemenc M, Strumbelj E (2015) Predicting the outcome of head-up tilt test using heart rate variability and baroreflex

sensitivity parameters in patients with vasovagal syncope. Clinical Autonomic Res 25(6):391–398
22. Kuran A, Erickson M, Petersen M, Franzen A, Williams T, Sutton R (2000) Respiratory changes in vasovagal syncope. J Cardiovasc Electrophysiol 11(6):607–611
23. Kurbaan A, Bowker T, Wijesekera N, Heaven D, Itty S, Sutton R (2003) Age and hemodynamic responses to tilt testing in those with syncope of unknown origin. J Am Coll Cardiol 41(6):1004–1007
24. Li H, Liao Y, Han Z, Wang Y, Liu P, Zhang C, Tang C, Du J, Jin H (2018) Head-up tilt test provokes dynamic alterations in total peripheral resistance and cardiac output in children with vasovagal syncope. Acta Paediatr 107(10):1786–1791
25. Mark A (1983) The bezold-jarisch reflex revisited: clinical implications of inhibitory reflexes originating in the heart. JAJCC 1(1):69–72
26. Mehlsen J, Kaijer M, Mehlsen AB (2008) Autonomic and electrocardiographic changes in cardioinhibitory syncope. Europace 10(1):91–95
27. Moya A, Sutton R, Ammirati F, Blanc JJ, Brignole M, Dahm J, Deharo JC, Gajek J, Gjesdal K, Krahn A, Massin M, Pepi M, Pezawas T, Ruiz Granell R, Sarasin F, Ungar A, van Dijk J, Walma E, Wieling W (2009) Guidelines for the diagnosis and management of syncope (version 2009). Europ Heart J 30:2631–2671
28. Ocon A, Medow M, Taneja I, Stewart J (2011) Respiration drives phase synchronization between blood pressure and rr interval following loss of cardiovagal baroreflex during vasovagal syncope. Am J Physiol 300(2):H527–H540
29. Parati G, Bretinieri M, Pomidossi G, Casadei R, Groppeli A, Pedotti A, Zanchetti A, Mancia G (1988) Evaluation of the baroreceptor-heart rate reflex by 24-hour intra-arterial blood pressure monitoring in humans. Hypertension 12(2):214–222
30. Parlow J, Viale J, Annat G, Hughson R, Quintin L (1995) Spontaneous cardiac baroreflex in humans: comparison with drug-induced responses. Hypertension 25(5):1058–1068
31. Probst M, Kanzaria H, Gbedemah M, Richardson L, Sun B (2015) National trends in resource utilization associated with ed visits for syncope. American. J Emergency Med 33(8):998–1001
32. Randall E, Billeschou A, Brinth L, Mehlsen J, Olufsen M (2019) A model-based analysis of autonomic nervous function in response to the valsalva maneuver. J Appl Physiol 127(5):1386–1402
33. Randall E, Randolph N, Olufsen M (2020) Persistent instability in a nonhomogeneous delay differential equation system of the valsalva maneuver. Math Biosci 319:108292
34. Remmen J, Aengevaeren W, Verheugt F, van ver Werf T, Luijten H, A Bos RJ (2002) Finapres arterial pulse wave analysis with modelflow is not a reliable non-invasive method for assessment of cardiac output. Clin Sci (Lond) 103(2):143–149
35. Robertson D, Biaggioni I, Low P (2011) Primer on the autonomic nervous system, 3rd edn. Elsevier, London
36. Romme J, van Dijk N, Boer K, Dekker L, Stam J, Reitsma J, Wieling W (2008) Influence of age and gender on the occurrence and presentation of reflex syncope. Clin Autonom Res 28(3):127–133
37. Rousseeuw P (1987) Silhouettes: a graphical aid to the interpretation and validation of cluster analysis. J Comp Appl Math 20:53–65
38. Sander-Jensen K, Mehlsen J, Stadeager C, Christensen N, Fahrenkrug J, Schwartz T, Warberg J, Bie P (1988) Increase in vagal activity during hypotensive lower-body negative pressure in humans. Am J Physiol 255(1 Pt 2):R149–R156
39. Sheldon R, Grubb B, Olshansky B (2015) 2015 heart rhythm society expert consensus statement on the diagnosis and treatment of postural tachycardia syndrome, inappropriate sinus tachycardia, and vasovagal syncope. Heart Rhythm 12(6):e41–e63
40. van Dijk J, Thijs R, Benditt D, Wieling W (2009) A guide to disorders causing transient loss of consciousness: focus on syncope. Nat Rev Neurol 5(8):438–448
41. Virag N, Sutton R, Vetter R, Markowitz T (2007) Prediction of vasovagal syncope from heart rate and blood pressure trend and variability: experience in 1,155 patients. Heart Rhythm 4(11):1375–1382
42. Vlasta B, Marchi A, De Maria B, Rossato G, Nollo G, Faes L, Porta A (2016) Nonlinear effects of respiration on the crosstalk between cardiovascular and cerebrovascular systems. Philos Trans A Math Phys Eng Sci 374(2067):2015079
43. Williams N, Wind-Willassen O, Wright A, Program R, Mehlsen J, Ottesen J, Olufsen M (2014) Patient-specific modelling of head-up tilt. Math Med Biol 31(4):365–392

Publisher's note Springer Nature remains neutral with regard to jurisdictional claims in published maps and institutional affiliations.

Steven Gilmore, PhD Student in Mathematics at NC State University. Contributed to writing the manuscript and was responsible for clustering and classification analysis.

Joseph Hart, PhD, Researcher at Sandia National Laboratories. Developed the machine learning classification methods for time-series data while he was a graduate student at NC State University.

Justen Geddes, PhD Student in Biomathematics at NC State University. Was responsible for ANOVA analysis, computed standard indices for baroreflex regulation, and contributed to clustering and classification analysis.

Christian H Olsen, PhD, Senior Statistical Programmer at Novo Nordisk, Denmark. Extracted and analyzed data from patient records and contributed to physiological interpretation of results from classification algorithms.

Jesper Mehlsen, MD, Surgical Pathophysiology, Rigshospitalet, University of Copenhagen. Was responsible for collecting data, providing expert classification, and interpretation of classification results.

Pierre Gremaud, PhD, Professor of Mathematics at NC State University. Expert in mathematical modeling and data analysis. Helped design the machine learning classification protocols used in this study.

Mette Olufsen, PhD, Professor of Mathematics at NC State University. Responsible for completing the manuscript, designing the study and interpreting the machine learning classification results.